Skeletal Radiol (2009) 38:751–760
DOI 10.1007/s00256-009-0682-1

SCIENTIFIC ARTICLE

Initial results of in vivo high-resolution morphological and biochemical cartilage imaging of patients after matrix-associated autologous chondrocyte transplantation (MACT) of the ankle

Sebastian Quirbach · Siegfried Trattnig · Stefan Marlovits · Valentin Zimmermann · Stephan Domayer · Ronald Dorotka · Tallal C. Mamisch · Klaus Bohndorf · Goetz H. Welsch

Received: 1 January 2009 / Revised: 22 February 2009 / Accepted: 2 March 2009 / Published online: 19 March 2009

Abstract
Objective The aim of this study was to use morphological as well as biochemical (T2 and T2* relaxation times and diffusion-weighted imaging (DWI)) magnetic resonance imaging (MRI) for the evaluation of healthy cartilage and cartilage repair tissue after matrix-associated autologous chondrocyte transplantation (MACT) of the ankle joint.

Materials and methods Ten healthy volunteers (mean age, 32.4 years) and 12 patients who underwent MACT of the ankle joint (mean age, 32.8 years) were included. In order to evaluate possible maturation effects, patients were separated into short-term (6–13 months) and long-term (20–54 months) follow-up cohorts. MRI was performed on a 3.0-T magnetic resonance (MR) scanner using a new dedicated eight-channel foot-and-ankle coil. Using high-resolution morphological MRI, the magnetic resonance observation of cartilage repair tissue (MOCART) score was assessed. For biochemical MRI, T2 mapping, T2* mapping, and DWI were obtained. Region-of-interest analysis was performed within native cartilage of the volunteers and control cartilage as well as cartilage repair tissue in the patients subsequent to MACT.

Results The overall MOCART score in patients after MACT was 73.8. T2 relaxation times (~50 ms), T2* relaxation times (~16 ms), and the diffusion constant for DWI (~1.3) were comparable for the healthy volunteers and the control cartilage in the patients after MACT. The cartilage repair tissue showed no significant difference in T2 and T2* relaxation times ($p \geq 0.05$) compared to the control cartilage; however, a significantly higher diffusivity (~1.5; $p < 0.05$) was noted in the cartilage repair tissue.

Conclusion The obtained results suggest that besides morphological MRI and biochemical MR techniques, such as T2 and T2* mapping, DWI may also deliver additional information about the ultrastructure of cartilage and cartilage repair tissue in the ankle joint using high-field MRI, a dedicated multichannel coil, and sophisticated sequences.

S. Quirbach · S. Trattnig (✉) · G. H. Welsch
MR Center—High-Field MR, Department of Radiology,
Medical University of Vienna, Vienna General Hospital,
Waehringer Guertel 18-20,
1090 Vienna, Austria
e-mail: siegfried.trattnig@meduniwien.ac.at

S. Marlovits · V. Zimmermann
Center for Joint and Cartilage, Department of Trauma Surgery,
Medical University of Vienna,
Vienna, Austria

S. Domayer · R. Dorotka
Department of Orthopedic Surgery, Medical University of Vienna,
Vienna, Austria

T. C. Mamisch
Department of Orthopedic Surgery, University of Berne,
Berne, Switzerland

K. Bohndorf
Department of Radiology, Klinikum Augsburg,
Augsburg, Germany

G. H. Welsch
Department of Trauma Surgery, University of Erlangen,
Erlangen, Germany

Keywords MRI · Ankle · MOCART · T2 · T2* · Diffusion-weighted imaging · MACT

Introduction

In joints with a high degree of curvature and a comparatively thin cartilage layer, such as the ankle joint, evaluation and detailed analysis of healthy cartilage and, even more importantly, degenerative or traumatic cartilage lesions are technically demanding [1]. The clinical impact of cartilage assessment is high since modern surgical therapies require an extensive preoperative diagnostic workup [2]. Therefore, it is necessary to consider new magnetic resonance imaging (MRI) techniques that potentially improve evaluation of anatomically challenging joints.

Cartilage repair techniques, especially microfracture and matrix-associated autologous chondrocyte transplantation (MACT), have been performed successfully in the ankle joint. Although the surgical procedure is more complex and technically demanding than MACT in the knee because of the different anatomy, several publications report good-to-excellent results for the postoperative outcome [3, 4].

The feasibility of 3.0-T MRI for the morphological imaging of the ankle or other small joints has been demonstrated in several studies [5–8]. Concerning the morphological evaluation of cartilage repair procedures, the magnetic resonance observation of cartilage repair tissue (MOCART) score is showing promising results in the knee joint [9, 10]. However, providing systematic cartilage repair assessment, it might be used for cartilage repair procedures also in the ankle joint [11]. In addition to morphological imaging, several methods that focus on direct visualization of cartilage structure and molecular composition in vivo have emerged using MRI [12–17]. Some of the most widely implemented biochemical MR techniques are delayed gadolinium-enhanced MRI of cartilage (dGEMRIC) and quantitative T2 mapping. Whereas dGEMRIC is seen to reflect the glycosaminoglycan content of cartilage, T2 is sensitive to collagen content and orientation, as well as hydration [12, 18, 19]. Recently, quantitative T2* mapping has been described for the evaluation of articular cartilage, with promising results [20, 21]. While T2* has been described as a technique near to T2, potential benefits due to faster scan times and 3D acquisition have been reported. Diffusion-weighted imaging (DWI), based on the translational movements of water protons [22], has also been reported as a novel technique in biochemical cartilage imaging. Initial studies have described the methods mentioned above as valuable imaging techniques in the knee joint [13, 23–26].

The purpose of the present study was to assess different quantitative MRI techniques in healthy volunteers, as well as in patients after MACT of the ankle joint. The focus was on evaluating quantitative T2 and T2* relaxation time values, as well as DWI of healthy articular cartilage and cartilage repair tissue of the ankle joint using a new dedicated foot-and-ankle coil. In patients after MACT of the ankle joint, the morphological constitution of the cartilage repair tissue was additionally assessed using the MOCART score.

Material and methods

Volunteers and patients

Ten healthy volunteers without known musculoskeletal disease and without a history of trauma or pain (mean age, 32.4 (standard deviation (SD) 11.2) years) and 12 patients who underwent MACT of the ankle joint (eight medial and four lateral talar dome) were included in the study. Patient age was 32.8 (SD 8.5) years and the cross-sectional postoperative follow-up was 19.8 (SD 12.6) months. Patients underwent cartilage transplantation surgery for a full-thickness cartilage defect caused by osteochondritis dissecans (OD) or trauma.

In order to evaluate potential effects of cartilage maturation over time, the patient group was divided based on postoperative interval to focus on possible effects due to repair tissue maturation. Thus, the patient group was divided into a short (6–13 months; n=6) and a long (20–54 months; n=6) follow-up interval. Detailed patient selection and data of all patients and of the two patient groups, regarding their postoperative interval, are displayed in Table 1.

The ethics commission of our university provided ethical approval for this study; prior to enrollment, written informed consent was obtained from all patients.

MR measurements

MRI was performed on a 3.0-T magnetic resonance (MR) scanner (Magnetom Trio, Siemens Medical Solutions, Erlangen, Germany) using a new eight-channel foot-and-ankle coil (InVivo, Gainesville, FL, USA). The subjects were placed in the supine position with the foot at a 90° angle relative to the lower leg. After localizing, MR sequences for morphological imaging were performed; in this study, an isotropic 3D True Fast Imaging with Steady-State Precession (3D-True-FISP) sequence was used, as well as a standard Proton-Density Fat-Suppressed Turbo-Spin-Echo (PD FS TSE) sequence. In healthy volunteers and patients, with the 3D-True-FISP sequence, the whole ankle joint was covered by 320 isotropic slices using a 160-mm field of view (FoV) and a 512^2 matrix, with an isotropic resolution of 0.31×

Table 1 Patient selection of all patients after matrix-associated autologous chondrocyte transplantation of the ankle joint (top) and further subdivision into two groups due to the postoperative interval (bottom)

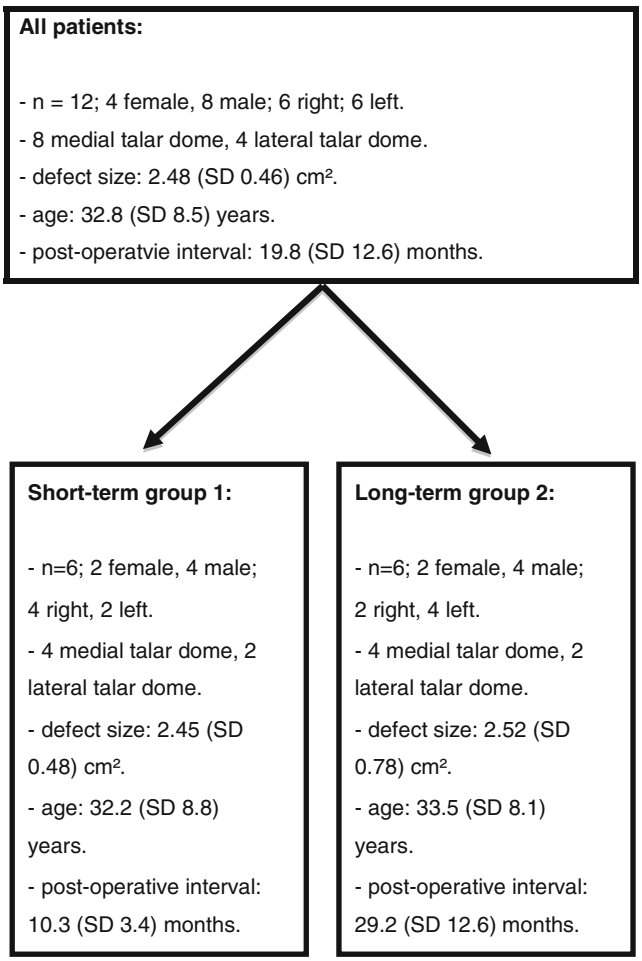

0.31×0.31 mm^3. Optimized sequence parameters for cartilage imaging at 3.0 T were used [8]. TR/TE was chosen with 9.65/4.18 ms, a flip angle of 28°, two averages, a bandwidth of 200 Hz/pixel and, by utilizing a parallel imaging technique (PAT) with an acceleration factor of three and a generalized autocalibrating partially parallel acquisition (GRAPPA) technique, scan time was set to 9:49 min. Parameters for the PD FS TSE sequence were as follows: TR/TE 2,400/39 ms; flip angle of 160°; one acquisition; PAT off; bandwidth of 244 Hz/pixel; and 16 slices, with a scan time of 4:02 min. The following biochemical T2 map, T2* map, and DWI sequences were obtained in the sagittal direction. In healthy volunteers, the sequences were planned on the medial talar dome using the 3D reconstruction of the isotropic True-FISP images. In the patient cohort, the exact localization of the following biochemical sequences was determined by the most central part of the cartilage repair area (i.e., medial or lateral talar dome). For all subsequent sequences, in-plane resolution was kept at 0.31×0.31 mm^2 and slice thickness was then set to 3 mm using a 100-mm FoV and a 320^2 matrix. Figure 1 visualizes morphological images (3D-True-FISP and PD FS TSE) of a patient after MACT of the medial talar dome.

Biochemical quantitative T2 imaging was obtained with a multiecho spin echo (ME-SE) T2 approach. Using six echoes, the measurement parameters were as follows: TE~ 16.5, 33.0, 49.5, 66.0, 82.5, 99.0 ms; TR 600 ms; flip angle 180°; two averages; PAT factor 2 using GRAPPA; bandwidth of 130 Hz/pixel; and ten slices in 10:53 min (Fig. 2).

T2* imaging was performed using a multiecho gradient recalled echo (ME-GRE) sequence, which also used six echoes (5.7, 9.8, 14.0, 18.1, 22.2, and 26.4 ms). TR was 177 ms, flip angle 35°, two averages, PAT off, bandwidth was 260 Hz/pixel, with ten slices, and total acquisition time was 7:28 min (Fig. 3).

For DWI, a three-dimensional, balanced, steady-state gradient echo pulse sequence with diffusion weighting (3D-DW reversed FISP (PSIF)) was used. The diffusion constant was assessed in "read" direction. Imaging parameters were as follows: TR=16.3 ms; TE=5.9 ms; flip angle=30°; 23 averages; PAT off; bandwidth 149 Hz/pixel; two slices; and the acquisition time for one sequence was 6:24 min.

In order to allow a semi-quantitative assessment of diffusional behavior in the cartilage, the diffusion sequence protocol consisted of two separate, but immediately consecutive, measurements using no (0) and 75 mT ms m^{-1} monopolar diffusion gradient moments for DWI and otherwise identical imaging parameters (Fig. 4). The presented DWI approach is semi-quantitative; therefore, only one direction is enough; however, it has to be seen as an estimation of quantitative diffusion values and has no *b* value or apparent diffusion constant (ADC) value.

Data analysis

In order to assess the morphological outcome in the patient after MACT of the ankle, the isotropic 3D-True-FISP sequence and the PD FS TSE sequence were used. Besides the standard PD FS TSE sequence, the True-FISP sequence has very recently been shown to achieve excellent results in the evaluation of articular cartilage [27–29]. The morphological condition of the cartilage repair tissue and the surrounding structures was evaluated by MOCART score [9, 10]. The MOCART score, as a point-scoring system was developed to assess different surgical cartilage repair procedures. The maximum score achievable in the evaluation of nine variables is 100. These variables are the degree of repair filling (1), the integration of the cartilage repair tissue to the border zone (2), the structure of the surface (3), the structure of the whole repair tissue (4), the signal intensity (5), the constitution of the subchondral lamina (6),

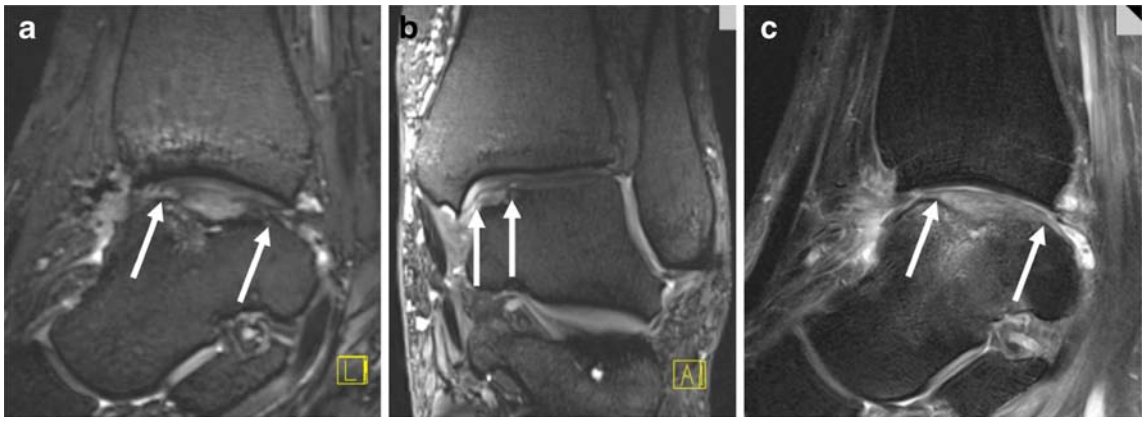

Fig. 1 Sagittal (**a**) and coronal (**b**) reconstruction of an isotropic 3D-True-FISP sequence and a sagittal (**c**) PD FS TSE sequence of a patient 12 months after MACT of the medial talar dome (*arrows*)

the constitution of the subchondral bone (7), possible adhesions (8), and possible effusion (9).

To evaluate the biochemical constitution of the repair tissue, T2 and T2* maps were obtained in-line using a pixel-wise, mono-exponential, non-negative least squares fit analysis (MapIt, Siemens Medical Solutions, Erlangen, Germany). For DWI, the PSIF images without a diffusion gradient were used for region-of-interest (ROI) data analysis; ROIs were then transferred onto the PSIF image with a diffusion gradient of 75 mT ms m^{-1} and without a diffusion gradient. Diffusion quotients were calculated by dividing the mean signal intensities in the ROIs on the PSIF images with a diffusion gradient by the corresponding ROI on the PSIF images without a diffusion gradient.

In all subjects enrolled in this study, the ROI analysis was performed on sagittal T2 and T2* maps, as well as on sagittal diffusion-weighted images. In all healthy volunteers, four ROIs were drawn in the cartilage layer along the curvature of the medial talar dome; in each subject, two consecutive slices were analyzed. In patients after MACT, the morphological 3D-True-FISP and the PD FS TSE images, as well as the surgical reports available at the time of MRI, determined the cartilage repair site. Two ROIs were drawn within the area of repair tissue, while another two ROIs covered healthy cartilage as an internal reference. An experienced senior musculoskeletal radiologist in consensus with an orthopedic surgeon with a special interest in musculoskeletal MRI drew the ROIs manually. For each ROI, mean T2 or T2* relaxation time or diffusion constant values, as well as standard deviation and number of pixels, were documented. Mean and SD values are given in the "Results" section; average number of pixels used for each ROI was 312 (SD 177).

Basic statistical evaluation was done for all volunteers (n=10), as well as for all patients (n=12). Quantitative evaluation of the biochemical T2, T2*, and DWI MR measurements was done by analysis of variance (ANOVA) using a three-way ANOVA with random factors, considering the fact of different measurements in each volunteer or patient. To gain as much information as possible from the biochemical evaluation, multiple ROIs where evaluated within each volunteer and each patient which bases the decision to use an analysis of variance. A separate statistical evaluation with regard to the different follow-up periods was only carried out for the morphological evaluation of the MOCART score. To assess differences between the short-term and the long-term follow-up groups, a double-tailed paired t test was used. Due to the small number of patients within these two groups, no further statistical evaluation was

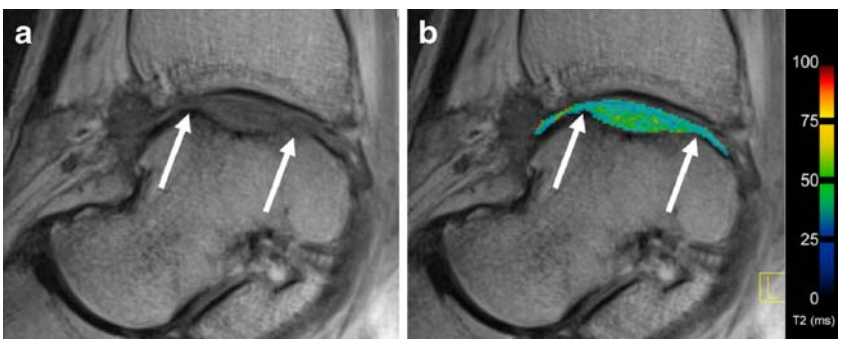

Fig. 2 Sagittal ME-SE sequence of the same patient (Fig. 1) after MACT of the ankle (*arrows*). A raw image (lowest echo time; **a**) as well as a cropped T2 map (**b**) shows homogeneous T2 values with only slight increase in the area of cartilage repair

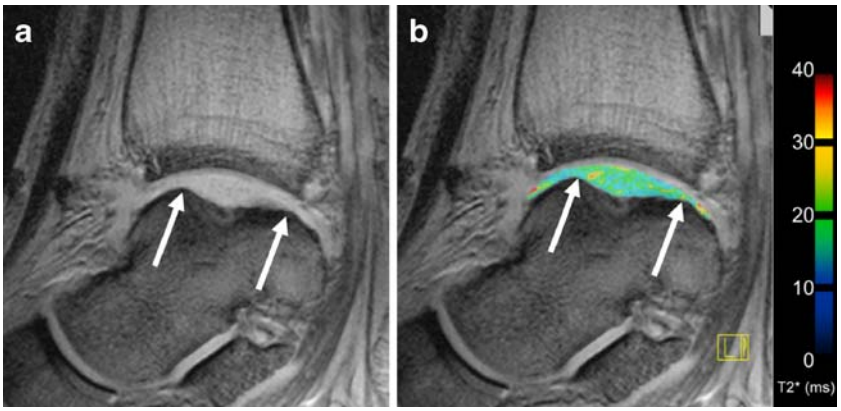

Fig. 3 Sagittal ME-GRE sequence of the same patient (Figs. 1 and 2) after MACT of the ankle (*arrows*). Comparable to Fig. 2, a raw image (lowest echo time; **a**) as well as a cropped T2 map (**b**) is visualizing the area of cartilage repair with similar relaxation times compared to the surrounding cartilage

prepared for the biochemical data. For the morphological and the biochemical evaluations of the two follow-up groups, results should only be seen descriptive. SPSS version 16.0 (SPSS Institute, Chicago, IL, USA) for Mac (Apple, Cupertino, CA, USA) was used. Differences with a P value less than 0.05 were considered statistically significant.

Results

Morphological evaluation

The overall MOCART score assessed for all patients after MACT of the ankle joint was 73.8 (SD 15.2). The different variables of this point scoring system are displayed in Table 2, where additionally the subdivision due to the postoperative follow-up is prepared. When comparing the groups with the shorter and the longer follow-up periods, the overall MOCART score increases from 66.7 (SD 12.9) to 80.8 (SD 14.9). This increase however was not statistically significant (p=0.109). The nine different variables show either similar or higher values in the patients with the longer follow-up period. Whereas the variables defect fill (p=0.780), integration of the cartilage repair tissue (p=1.000), surface (p=1.000), structure (p=0.290), subchondral lamina (p=0.549), subchondral bone (p=0.341), adhesions (p=1.000), and effusion (p=0.260) showed no significant difference, the signal intensity of the repair tissue was charged significantly better within the longer follow-up (0.018).

Biochemical evaluation

Mean T2 relaxation time for all healthy volunteers in articular cartilage on the trochlear surface of the talus was 51.1 ms (SD 4.6). For T2*, mean relaxation time was 16.6 ms (SD 3.7). The diffusion constant on diffusion-weighted images was 1.27 (SD 0.16). For healthy control areas in patients after MACT, mean T2 value was 47.6 (SD 9.3); mean T2* was 15.8 (SD 3.6), and the diffusion constant was 1.28 (SD 0.17). There was no significant difference ($p \geq 0.05$) between cartilage in volunteers and healthy control cartilage in patients after MACT. In cartilage repair tissue in patients after MACT, mean T2 values were 50.1 (SD 8.0); mean T2* values were 17.3 (SD 4.6), and the diffusion constant was 1.49 (SD 0.32). For T2 and T2* values, no significant difference between cartilage repair tissue and healthy cartilage could be observed (p=

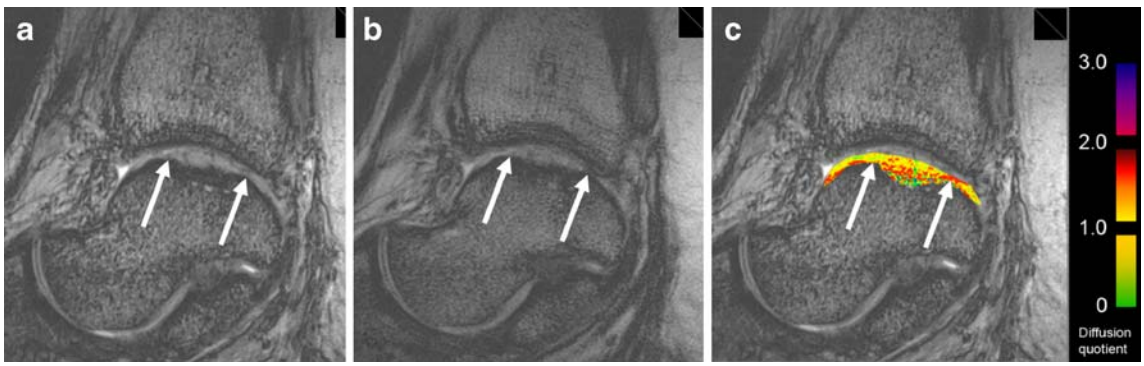

Fig. 4 Sagittal three-dimensional, balanced, steady-state gradient echo pulse sequence with diffusion weighting (3D-DW PSIF; reversed FISP) of the same patient (Figs. 1, 2, and 3) after MACT of the ankle (*arrows*). The presented images using no (**a**) and 75 mT ms m^{-1} (**b**) monopolar diffusion gradient moments for DWI. The DWI map (**c**) marks higher diffusivity in the area of cartilage repair compared to the surrounding cartilage

Table 2 Morphological MRI evaluation of cartilage repair tissue in all patients after MACT of the ankle joint (n=12) using the MOCART score

Variables	All patients	Short term	Long term
Degree of defect repair and filling of the defect			
Complete (20)	7 (58)	4 (67)	3 (50)
Hypertrophy (15)	1 (8)	0 (0)	1 (17)
Incomplete			
>50% of the adjacent cartilage (10)	4 (33)	2 (33)	2 (33)
<50% of the adjacent cartilage (5)	0 (0)		
Subchondral bone exposed (0)	0 (0)		
Integration to border zone			
Complete (15)	8 (67)	4 (67)	4 (67)
Incomplete			
Demarcating border visible (slit like; 10)	4 (33)	2 (33)	2 (33)
Defect visible <50% of the length (5)	0 (0)		
Defect visible >50% of the length (0)	0 (0)		
Surface of the repair tissue			
Surface intact (10)	10 (83)	5 (83)	5 (83)
Surface damaged <50% of depth (5)	2 (17)	1 (17)	1 (17)
Surface damaged >50% of depth (0)	0 (0)		
Structure of the repair tissue			
Homogeneous (5)	6 (50)	2 (33)	4 (67)
Inhomogeneous (0)	6 (50)	4 (67)	2 (33)
Signal intensity of the repair tissue			
Normal (identical to adjacent cartilage; 30)	6 (50)	1 (17)	5 (83)
Nearly normal (slight areas of signal alteration; 15)	6 (50)	5 (83)	1 (17)
Abnormal (large areas of signal alteration; 0)	0 (0)		
Subchondral lamina			
Intact (5)	3 (25)	1 (17)	2 (33)
Not intact (0)	9 (75)	5 (83)	4 (67)
Subchondral bone			
Intact (5)	1 (8)	0 (0)	1 (17)
Not intact (0)	11 (92)	6 (100)	5 (83)
Adhesions			
No (5)	12 (100)	6 (100)	6 (100)
Yes (0)	0 (0)		
Effusion			
No (5)	8 (67)	3 (50)	5 (83)
Yes (0)	4 (33)	3 (50)	1 (17)

Further subdivision in a short-term (n=6) and a long-term (n=6) postoperative interval. Values by number of patients and percentage within the group

Table 3 Biochemical T2 (ms), T2* (ms), and diffusion-weighted (DWI index) values of the patients after MACT of the ankle joint

Therapy		T2	T2*	DWI
Cartilage repair tissue	Mean	50.1	17.3	1.49
	SD	8.0	4.6	0.32
Control cartilage	Mean	47.6	15.8	1.28
	SD	9.3	3.6	0.17

Values are given for all patients (n=12)

0.379 for T2 and p=0.259 for T2*). The diffusion constant, however, showed a significant difference between repair tissue and healthy control areas in patients (p=0.039). Mean values and SD are depicted in Table 3.

With regard to the postoperative follow-up, because of the small groups and the relatively inhomogeneous follow-up periods, biochemical data are merely descriptive. Within the short follow-up period of 6–13 months, T2 and T2* relaxation times were longer for cartilage repair tissue compared to the control cartilage. T2 and T2* measurements within the longer follow-up period of 20–54 months, in contrast, showed equal values for cartilage repair tissue

and healthy control cartilage in patients. The diffusion constant showed, for both the shorter and the longer follow-up periods, higher diffusivity in the cartilage repair tissue compared to the control cartilage. This difference, however, was more pronounced in the shorter follow-up period. The values for the different follow-up periods are displayed in Table 4.

Discussion

With the present study, advanced morphological and biochemical MRI of the ankle joint are presented in healthy volunteers and patients after MACT of the talar dome. Morphological MOCART scoring was prepared in the patient group and mean MOCART values were comparable to the knee joint. Whereas Trattnig et al. [30] report a score of 73 in patients 12 months after a comparable cartilage repair procedure in the knee, Welsch et al. [31] depict scores of 73 for the patella and 72 for the medial femoral condyle in a cross-sectional evaluation with a mean of 29 months after MACT. Remarkably, it however remains that, in our study after MACT of medial and lateral talar dome, the repair filling and the integration of the repair tissue showed relatively good results, whereas the subchondral lamina and the subchondral bone seemed to be abnormal in nearly all patients. This might be due to the natural course of the cartilage defect in the talar dome, in most cases caused by OD.

With regard to T2 mapping, the reported mean relaxation time values of the cartilage repair tissue and the healthy control cartilage were similar to those found in the knee using comparable T2 techniques [32, 33]. However, existing studies using quantitative T2 in the follow-up after cartilage transplantation show clearly higher T2 values in the first year after surgery for the repair tissue adapting over time to the values of the surrounding control cartilage [32, 34]. Hence one main goal of T2 mapping on the knee had been to utilize this technique as a tool for monitoring the maturation of cartilage repair tissue. An in vitro study by Watrin-Pinzano et al. [15] and recent initial in vivo studies [32, 34] report this ability of quantitative T2. The initial high T2 values are seen to reflect higher hydration and immature collagen composition; over time, the cartilage repair tissue shows an ideally "hyaline-like" structure and T2 values assimilate to the surrounding healthy cartilage. In the present study, the higher T2 values in cartilage repair tissue at the shorter postoperative follow-up and the subsequent return to the values of control cartilage in the longer follow-up may support the assumption of cartilage repair tissue maturation. The low patient number and the cross-sectional character of the study however may limit this proposition; furthermore, these results are only descriptive and no statistical evaluation or significances have been carried out due to the small number of patients. The validity of T2 mapping in the knee has been confirmed by several publications [16, 18, 35–40]; the same technique appears to be also feasible in the ankle [8]. In our study, T2 mapping was able to depict articular cartilage in healthy volunteers and healthy control cartilage as well as cartilage repair tissue in the ankle joint; therefore, T2 mapping appears to be a suitable method for imaging of smaller joints as well. The absolute T2 value however should not be used to characterise the quality of cartilage repair tissue. In vitro and in vivo studies show varying results [15, 16, 31, 33, 34, 41–43] and the use of increasing or decreasing T2 values in the larger field of osteoarthritis is further discussed [36]. Hence, the T2 values of the cartilage repair tissue have always to be compared to the surrounding control cartilage. In the knee joint, zonal T2 evaluation has shown promising results [44]. Spatial variation, imaged as an increase in T2 values from the deep to the superficial zone, reflects the collagen fiber orientation of hyaline cartilage and seems to correspond to the appearance of hyaline-like cartilage structure after cartilage repair [16]. In the ankle, however, we found a zonal evaluation impractical because of the thin cartilage layer and the overall challenging anatomy. Even with high magnetic field strength and high-resolution sequences, the small-scale anatomy of the talar trochlea could not be depicted in a way that would allow the

Table 4 Biochemical T2 (ms), T2* (ms), and diffusion-weighted (DWI index) values of the patients after MACT of the ankle due to their postoperative interval

Postoperative interval	Therapy		T2	T2*	DWI
6–13 months	Cartilage repair tissue	Mean	54.4	17.1	1.67
		SD	8.7	6.3	0.38
	Control cartilage	Mean	49.7	15.1	1.38
		SD	8.1	2.0	0.19
20–54 months	Cartilage repair tissue	Mean	46.3	17.4	1.36
		SD	5.1	3.0	0.22
	Control cartilage	Mean	46.0	16.2	1.23
		SD	10.2	4.3	0.13

assessment of zonal differences. This will remain challenging for future approaches.

In recent studies, T2* mapping has been described as a valuable tool in cartilage imaging [20, 21]. The only published study using exactly the same approach for T2* mapping showed promising results at ultrahigh fields [45]. In our study, the absolute mean relaxation time values found in T2* mapping were lower than in T2 mapping; this was to be expected due to the technical nature of the T2* sequence. With regard to the comparison between healthy control cartilage in patients and cartilage repair tissue, T2* showed tendencies similar to T2. Comparable to T2 relaxation, also for T2* relaxation, initial studies show the importance of zonal analysis of healthy articular cartilage and cartilage repair tissue, particularly because of the close association of zonal variation in T2 values with the appearance of hyaline cartilage [46, 47]. Again, this will be challenging for future approaches, even at potentially higher resolution. A very recent study suggested that, due to the potentially shorter scan times, T2* can be regarded as a fast T2 mapping technique [21]. Although we would postulate T2* more as an extra biomarker in addition to standard T2, it may, in future, possibly attain a high enough resolution and signal in a clinically practical scan time to enable zonal assessment in the ankle joint. With the present study, the possibility of T2* mapping in the ankle has been demonstrated. Future studies, however, will have to validate this mapping technique in detail.

Our results for diffusion-weighted imaging (DWI) in the ankle have demonstrated it to be a promising novel approach. Similar to T2 and T2* mapping, recent studies have demonstrated good initial results regarding the feasibility of DWI for the biochemical imaging of healthy cartilage, as well as for the biochemical assessment of cartilage repair tissue in the knee [26]. One major aspect of DWI is the ability to distinguish areas of healthy hyaline cartilage from cartilage repair tissue in the ankle joint, even after long postoperative intervals. Using T2 and T2* alone, no differences between healthy and repair tissue were detected; an analysis of the mean relaxation values did not reveal any significant differences. Regarding the diffusion constant, however, a significant difference between healthy control cartilage in patients after MACT and cartilage repair tissue was detected. In addition, the decrease of diffusivity over time may actually signify the maturation of cartilage repair tissue. The time period for this cartilage repair tissue maturation is seen to be around 12 months [26, 48]. A clear difference between quantitative T2 and DWI concerning the maturation of cartilage repair tissue is that over time T2 values adapt to those of the internal control cartilage, whereas the DWI values of cartilage repair tissue seem to remain higher compared to the control cartilage and, even after a longer period of time, the diffusivity of the repair tissue is not comparable to healthy cartilage. The results from the present study demonstrated the basic feasibility of DWI for cartilage imaging in smaller joints, such as the ankle. In future studies, however, the focus will have to be shifted from semi-quantitative mapping techniques to analysis of ADC values. With this method, true quantitative evaluation of biochemical cartilage imaging based on DWI is possible.

One major limitation of our study was the relatively small cohort of patients, which may reduce the actual clinical impact. However, since this therapy option is rarely used in the ankle joint, the existing small cohort may help to elucidate the potential of biochemical imaging in the ankle joint. The lack of uniform follow-up periods is clearly a limitation to the present study. The cross-sectional evaluation may, in particular, limit the ability to draw conclusions from the presented results. The further evaluation of two groups concerning their postoperative follow-up intervals is seen as only descriptive in nature. Another limiting factor is the lack of histological and clinical confirmation of the radiological evaluation. A further limitation is that since most of the cartilage repair areas in patients were located on the medial talar dome, we determined the control ROIs in volunteers only on the medial talar dome and hence their validity concerning the lateral talar dome may be limited. Concerning the single sequences, it has to be stated as limitations that T2* mapping and the presented DWI approach lack histological validation studies like they are available for T2 [49, 50]. Furthermore single parameters have to be evaluated for these new methodologies like, e.g., TR for T2* relaxation and diffusion gradient and direction for DWI. The semi-quantitative nature of the DWI approach and the consecutive lack of a *b* value or ADC values is a further limitation. Nevertheless, the presented semi-quantitative DWI approach gains high enough signal-to-noise ratio, low artifacts, and high resolution to be obtained in vivo at the relatively thin talar cartilage in a clinically applicable scan time.

To the best of our knowledge, this is the first study to focus on the biochemical imaging of the talocrural joint in patients after MACT. Utilizing experience gained from biochemical cartilage imaging in the knee, we were able to demonstrate the feasibility of this technique for smaller joints with a technically challenging anatomic structure, such as the ankle. With the advances in high-resolution imaging, the difficulties imposed by anatomy can be overcome. The data we obtained suggest that T2 and T2* mapping techniques, as well as diffusion-weighted imaging, provide additional information about the ultrastructure of healthy articular cartilage and cartilage repair tissue in a clinically practical scan time using high-field (3 T) MRI, a dedicated multichannel coil, and sophisticated sequences. The imaging techniques covered by our study may, in the future, provide excellent tools for the diagnosis, grading, and postoperative follow-up of cartilage lesions in the ankle joint.

Acknowledgements Funding for this study was provided by Austrian Science Fund (FWF) FWF-TRP-Projekt L243-B15.

References

1. Millington SA, Li B, Tang J, et al. Quantitative and topographical evaluation of ankle articular cartilage using high resolution MRI. J Orthop Res. 2007; 25: 143–151.
2. Hangody L, Fules P. Autologous osteochondral mosaicplasty for the treatment of full-thickness defects of weight-bearing joints: ten years of experimental and clinical experience. J Bone Joint Surg Am. 2003; 85-A(Suppl 2): 25–32.
3. Giannini S, Buda R, Vannini F, Di Caprio F, Grigolo B. Arthroscopic autologous chondrocyte implantation in osteochondral lesions of the talus: surgical technique and results. Am J Sports Med. 2008; 36: 873–880.
4. Whittaker JP, Smith G, Makwana N, et al. Early results of autologous chondrocyte implantation in the talus. J Bone Joint Surg Br. 2005; 87: 179–183.
5. Bolog N, Nanz D, Weishaupt D. Musculoskeletal MR imaging at 3.0T: current status and future perspectives. Eur Radiol. 2006; 16: 1298–1307.
6. Mosher TJ. Musculoskeletal imaging at 3T: current techniques and future applications. Magn Reson Imaging Clin N Am. 2006; 14: 63–76.
7. Ramnath RR. 3T MR imaging of the musculoskeletal system (part II): clinical applications. Magn Reson Imaging Clin N Am. 2006; 14: 41–62.
8. Welsch GH, Mamisch TC, Weber M, Horger W, Bohndorf K, Trattnig S. High-resolution morphological and biochemical imaging of articular cartilage of the ankle joint at 3.0T using a new dedicated phased array coil: in vivo reproducibility study. Skeletal Radiol. 2008; 37: 519–526.
9. Marlovits S, Singer P, Zeller P, Mandl I, Haller J, Trattnig S. Magnetic resonance observation of cartilage repair tissue (MOCART) for the evaluation of autologous chondrocyte transplantation: determination of interobserver variability and correlation to clinical outcome after 2 years. Eur J Radiol. 2006; 57: 16–23.
10. Marlovits S, Striessnig G, Resinger CT, et al. Definition of pertinent parameters for the evaluation of articular cartilage repair tissue with high-resolution magnetic resonance imaging. Eur J Radiol. 2004; 52: 310–319.
11. Choi YS, Potter HG, Chun TJ. MR imaging of cartilage repair in the knee and ankle. Radiographics. 2008; 28: 1043–1059.
12. Burstein D, Velyvis J, Scott KT, et al. Protocol issues for delayed Gd(DTPA)(2-)-enhanced MRI: (dGEMRIC) for clinical evaluation of articular cartilage. Magn Reson Med. 2001; 45: 36–41.
13. Miller KL, Hargreaves BA, Gold GE, Pauly JM. Steady-state diffusion-weighted imaging of in vivo knee cartilage. Magn Reson Med. 2004; 51: 394–398.
14. Trattnig S, Millington SA, Szomolanyi P, Marlovits S. MR imaging of osteochondral grafts and autologous chondrocyte implantation. Eur Radiol. 2007; 17: 103–118.
15. Watrin-Pinzano A, Ruaud JP, Cheli Y, et al. Evaluation of cartilage repair tissue after biomaterial implantation in rat patella by using T2 mapping. Magn Reson Mater Phy. 2004; 17: 219–228.
16. White LM, Sussman MS, Hurtig M, Probyn L, Tomlinson G, Kandel R. Cartilage T2 assessment: differentiation of normal hyaline cartilage and reparative tissue after arthroscopic cartilage repair in equine subjects. Radiology. 2006; 241: 407–414.
17. Williams A, Gillis A, McKenzie C, et al. Glycosaminoglycan distribution in cartilage as determined by delayed gadolinium-enhanced MRI of cartilage (dGEMRIC): potential clinical applications. Am J Roentgenol. 2004; 182: 167–172.
18. Glaser C. New techniques for cartilage imaging: T2 relaxation time and diffusion-weighted MR imaging. Radiol Clin North Am. 2005; 43: 641–653. vii.
19. Mosher TJ, Dardzinski BJ. Cartilage MRI T2 relaxation time mapping: overview and applications. Semin Musculoskelet Radiol. 2004; 8: 355–368.
20. Murphy BJ. Evaluation of grades 3 and 4 chondromalacia of the knee using T2*-weighted 3D gradient-echo articular cartilage imaging. Skeletal Radiol. 2001; 30: 305–311.
21. Quaia E, Toffanin R, Guglielmi G, et al. Fast T2 mapping of the patellar articular cartilage with gradient and spin-echo magnetic resonance imaging at 1.5T: validation and initial clinical experience in patients with osteoarthritis. Skeletal Radiol. 2008; 37: 511–517.
22. Szafer A, Zhong J, Anderson AW, Gore JC. Diffusion-weighted imaging in tissues: theoretical models. NMR Biomed. 1995; 8: 289–296.
23. Miller KL, Pauly JM. Nonlinear phase correction for navigated diffusion imaging. Magn Reson Med. 2003; 50: 343–353.
24. Mlynarik V, Sulzbacher I, Bittsansky M, Fuiko R, Trattnig S. Investigation of apparent diffusion constant as an indicator of early degenerative disease in articular cartilage. J Magn Reson Imaging. 2003; 17: 440–444.
25. Recht MP, Goodwin DW, Winalski CS, White LM. MRI of articular cartilage: revisiting current status and future directions. AJR Am J Roentgenol. 2005; 185: 899–914.
26. Mamisch TC, Menzel MI, Welsch GH, et al. Steady-state diffusion imaging for MR in-vivo evaluation of reparative cartilage after matrix-associated autologous chondrocyte transplantation at 3 Tesla—preliminary results. Eur J Radiol. 2008; 65: 72–79.
27. Duc SR, Koch P, Schmid MR, Horger W, Hodler J, Pfirrmann CW. Diagnosis of articular cartilage abnormalities of the knee: prospective clinical evaluation of a 3D water-excitation true FISP sequence. Radiology. 2007; 243: 475–482.
28. Duc SR, Pfirrmann CW, Koch PP, Zanetti M, Hodler J. Internal knee derangement assessed with 3-minute three-dimensional isovoxel true FISP MR sequence: preliminary study. Radiology. 2008; 246: 526–535.
29. Duc SR, Pfirrmann CW, Schmid MR, et al. Articular cartilage defects detected with 3D water-excitation true FISP: prospective comparison with sequences commonly used for knee imaging. Radiology. 2007; 245: 216–223.
30. Trattnig S, Ba-Ssalamah A, Pinker K, Plank C, Vecsei V, Marlovits S. Matrix-based autologous chondrocyte implantation for cartilage repair: noninvasive monitoring by high-resolution magnetic resonance imaging. Magn Reson Imaging. 2005; 23: 779–787.
31. Welsch GH, Mamisch TC, Quirbach S, Zak L, Marlovits S, Trattnig S (2008) Evaluation and comparison of cartilage repair tissue of the patella and medial femoral condyle by using morphological MRI and biochemical zonal T2 mapping. Eur Radiol (in press)
32. Trattnig S, Mamisch TC, Welsch GH, et al. Quantitative T2 mapping of matrix-associated autologous chondrocyte transplantation at 3 Tesla: an in vivo cross-sectional study. Invest Radiol. 2007; 42: 442–448.
33. Welsch GH, Mamisch TC, Domayer SE, et al. Cartilage T2 assessment at 3-T MR imaging: in vivo differentiation of normal hyaline cartilage from reparative tissue after two cartilage repair procedures—initial experience. Radiology. 2008; 247: 154–161.
34. Welsch GH, Mamisch TC, Marlovits S, et al. (2009) Quantitative T2 mapping during follow-up after matrix-associated autologous chondrocyte transplantation (MACT): full-thickness and zonal evaluation to visualize the maturation of cartilage repair tissue. J Orthop Res (in press)
35. Mosher TJ, Smith HE, Collins C, et al. Change in knee cartilage T2 at MR imaging after running: a feasibility study. Radiology. 2005; 234: 245–249.

36. Burstein D, Gray ML. Is MRI fulfilling its promise for molecular imaging of cartilage in arthritis? Osteoarthr Cartil. 2006; 14: 1087–1090.
37. Nieminen MT, Rieppo J, Toyras J, et al. T2 relaxation reveals spatial collagen architecture in articular cartilage: a comparative quantitative MRI and polarized light microscopic study. Magn Reson Med. 2001; 46: 487–493.
38. Dunn TC, Lu Y, Jin H, Ries MD, Majumdar S. T2 relaxation time of cartilage at MR imaging: comparison with severity of knee osteoarthritis. Radiology. 2004; 232: 592–598.
39. Wayne JS, Kraft KA, Shields KJ, Yin C, Owen JR, Disler DG. MR imaging of normal and matrix-depleted cartilage: correlation with biomechanical function and biochemical composition. Radiology. 2003; 228: 493–499.
40. Watrin-Pinzano A, Ruaud JP, Cheli Y, et al. Evaluation of cartilage repair tissue after biomaterial implantation in rat patella by using T2 mapping. Magma. 2004; 17: 219–228.
41. Domayer SE, Kutscha-Lissberg F, Welsch G, et al. T2 mapping in the knee after microfracture at 3.0T: correlation of global T2 values and clinical outcome—preliminary results. Osteoarthr Cartil. 2008; 16: 903–908.
42. Domayer SE, Welsch GH, Nehrer S, et al. (2009) T2 mapping and dGEMRIC after autologous chondrocyte implantation with a fibrin-based scaffold in the knee: preliminary results. Eur J Radiol (in press)
43. Welsch GH, Trattnig S, Scheffler K, et al. Magnetization transfer contrast and T2 mapping in the evaluation of cartilage repair tissue with 3T MRI. J Magn Reson Imaging. 2008; 28: 979–986.
44. Smith HE, Mosher TJ, Dardzinski BJ, et al. Spatial variation in cartilage T2 of the knee. J Magn Reson Imaging. 2001; 14: 50–55.
45. Welsch GH, Mamisch TC, Hughes T, et al. In vivo biochemical 7.0 Tesla magnetic resonance: preliminary results of dGEMRIC, zonal T2, and T2* mapping of articular cartilage. Invest Radiol. 2008; 43: 619–626.
46. Hughes T, Welsch GH, Trattnig S, Brandi L, Domayer S, Mamisch TC. T2-star relaxation as a means to differentiate cartilage repair tissue after microfracturing therapy. Intern Soc Magn Reson Med. 2007; 15: 183.
47. Welsch GH, Hughes T, Quirbach S, et al. T2 and T2* relaxation as a means to evaluate cartilage repair tissue—initial results. Intern Soc Magn Reson Med. 2008; 16: 216.
48. Friedrich KM, Mamisch TC, Plank C, et al. (2009) Diffusion-weighted imaging for the follow-up of patients after matrix-associated autologous chondrocyte transplantation. Eur J Radiol (in press)
49. Goodwin DW, Wadghiri YZ, Dunn JF. Micro-imaging of articular cartilage: T2, proton density, and the magic angle effect. Acad Radiol. 1998; 5: 790–798.
50. Xia Y, Moody JB, Alhadlaq H. Orientational dependence of T2 relaxation in articular cartilage: a microscopic MRI (microMRI) study. Magn Reson Med. 2002; 48: 460–469.